

0.1 Residual Correlations

The purpose of this analysis is to study both the interaction, and the scale of the emitting source, of the pairs. In order to obtain correct results, it is important for our particle collections to consist of primary particles. In practice, this is difficult to achieve for our Λ and $\bar{\Lambda}$ collections. Many of our Λ particles are not primary, but originate as decay products from other hyperons, including Σ^0 , Ξ^0 , Ξ^- and $\Sigma^{*(+,-,0)}$ (1385). Additionally, many of our K particles are not primary, but decay from $K^{*(+,-,0)}$ (892) parents. In these decays, the daughter Λ or K_S^0 carries away a momentum very similar to that of its parent. As a result, the correlation function between a secondary Λ and, for instance, a K^+ will be sensitive to, and dependent upon, the interaction between the parent of the Λ and the K^+ . In effect, the correlation between the parent of the Λ and the K^+ (ex. $\Sigma^0 K^+$) will be visible, although smeared out, in the ΛK^+ data; we call this a residual correlation resulting from feed-down. The contributions from the primary correlation, residual correlations, and fake pairs on the finally measure data is shown schematically in Figure 1. Residual correlations are important in an analysis when three criteria are met [?]: i) the parent correlation signal is large, ii) a large fraction of pairs in the sample originate from the particular parent system, and iii) the decay momenta are comparable to the expected correlation width in k^* .

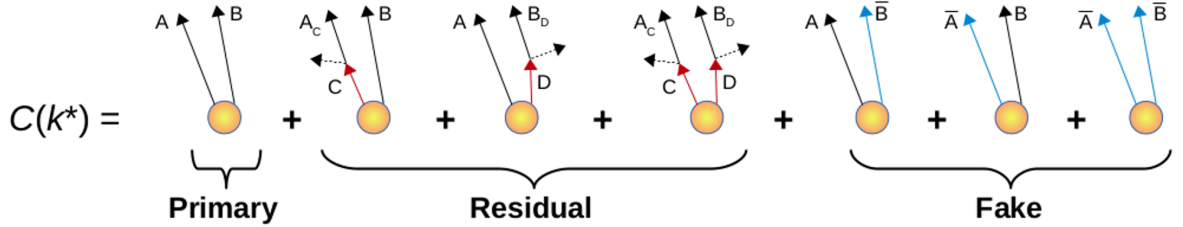


Fig. 1: A schematic representation of the contributions to the finally measured data from the primary correlation, residual correlations, and fake pairs.

As it is difficult for us to eliminate these residual correlations in our analyses, we must attempt to account for them in our fit. To achieve this, we will simultaneously fit the data for both the primary correlation function and the residual correlations. For example, in the simple case of a ΛK^+ analysis with residuals arising solely from $\Sigma^0 K^+$ feed-down:

$$C_{measured}(k_{\Lambda K^+}^*) = 1 + \lambda_{\Lambda K^+} [C_{\Lambda K^+}(k_{\Lambda K^+}^*) - 1] + \lambda_{\Sigma^0 K^+} [C_{\Sigma^0 K^+}(k_{\Lambda K^+}^*) - 1]$$

$$C_{\Sigma^0 K^+}(k_{\Lambda K^+}^*) \equiv \frac{\sum_{k_{\Sigma^0 K^+}^*} C_{\Sigma^0 K^+}(k_{\Sigma^0 K^+}^*) T(k_{\Sigma^0 K^+}^*, k_{\Lambda K^+}^*)}{\sum_{k_{\Sigma^0 K^+}^*} T(k_{\Sigma^0 K^+}^*, k_{\Lambda K^+}^*)} \quad (1)$$

$C_{\Sigma^0 K^+}(k_{\Sigma^0 K^+}^*)$ is the $\Sigma^0 K^+$ correlation function from, for instance, Equation ??, and T is the transform matrix generated with THERMINATOR. The transform matrix is formed for a given parent pair, AB , by taking all ΛK pairs originating from AB , calculating the relative momentum of the parents (k_{AB}^*) and daughters ($k_{\Lambda K}^*$), and filling a two-dimensional histogram with the values. The transform matrix is essentially an unnormalized probability distribution mapping the k^* of the parent pair to that of the daughter pair when one or both parents decay. An example of such transform matrices can be found in Figures 2 and 3.

The above equation can be easily extended to include feed-down from more sources:

$$\begin{aligned}
C_{measured}(k_{\Lambda K}^*) &= 1 + \lambda_{\Lambda K}[C_{\Lambda K}(k_{\Lambda K}^*) - 1] + \lambda_{\Sigma^0 K}[C_{\Sigma^0 K}(k_{\Lambda K}^*) - 1] + \dots \\
&\quad + \lambda_{P_1 P_2}[C_{P_1 P_2}(k_{\Lambda K}^*) - 1] + \lambda_{other}[C_{other}(k_{\Lambda K}^*) - 1] \\
C_{P_1 P_2}(k_{\Lambda K}^*) &\equiv \frac{\sum_{k_{P_1 P_2}^*} C_{P_1 P_2}(k_{P_1 P_2}^*) T(k_{P_1 P_2}^*, k_{\Lambda K}^*)}{\sum_{k_{P_1 P_2}^*} T(k_{P_1 P_2}^*, k_{\Lambda K}^*)}
\end{aligned} \tag{2}$$

Or, more compactly:

$$C_{measured}(k_{\Lambda K}^*) = 1 + \sum_i \lambda_i [C_i(k_{\Lambda K}^*) - 1] \tag{3}$$

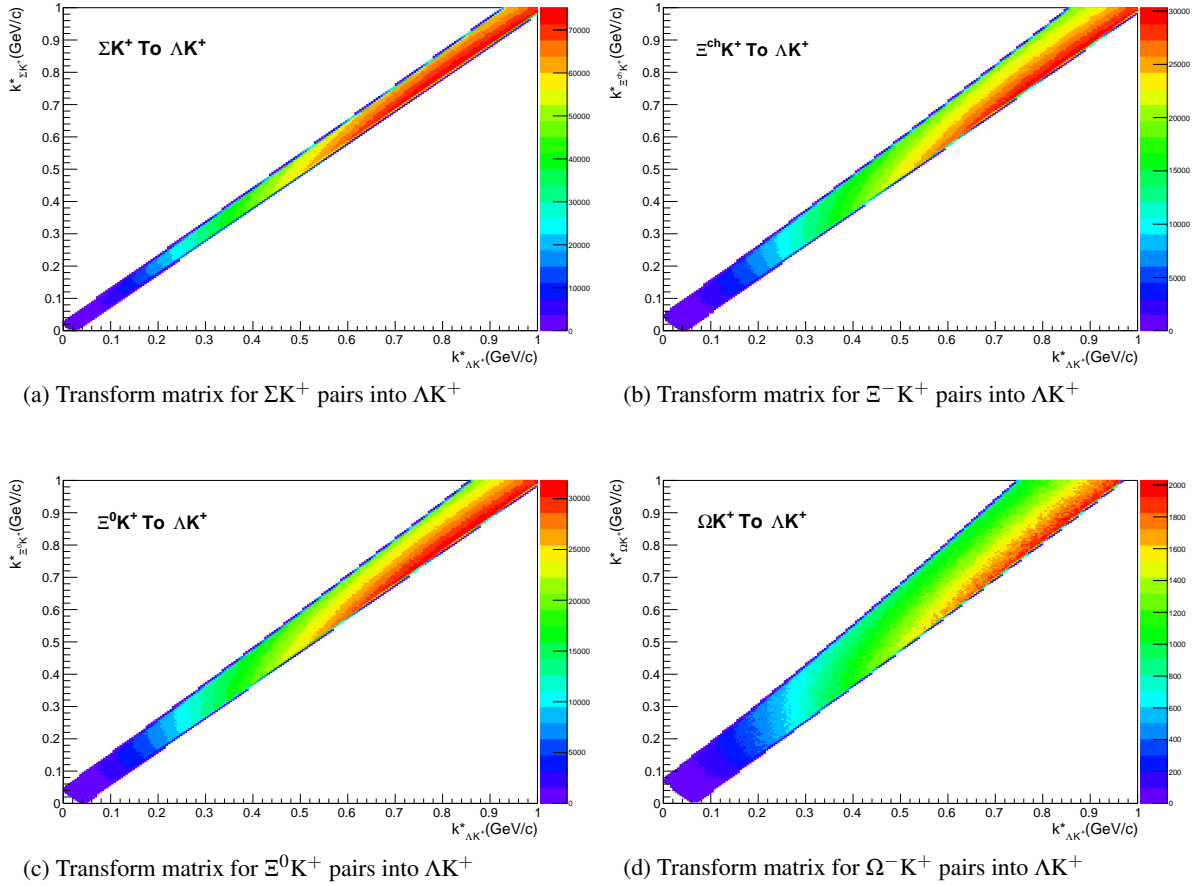


Fig. 2: Sample Transform Matrices generated with THERMINATOR for ΛK^+ Analysis

So, in practice, we model the correlation function of the parents (ex. $\Sigma^0 K^+$), and run the correlation function through the appropriate transform matrix to determine the contribution to the daughter correlation function (ex. ΛK^+). A few questions still remain. First, what λ values should be used in the above equation? One option would be to leave all of these λ -parameters free during the fit process. However, this would introduce a huge number of new parameters into the fitter, and would make the fit results less trustworthy. The λ parameters roughly dictate the strength of the parent contribution to the daughter pair. Additionally, as found in [?], the reconstruction efficiency for primary Λ particles is nearly equal to that of Λ particles originating from Σ , Σ^* , Ξ^0 , Ξ^- , and Ω hyperons. Therefore, the λ parameter for

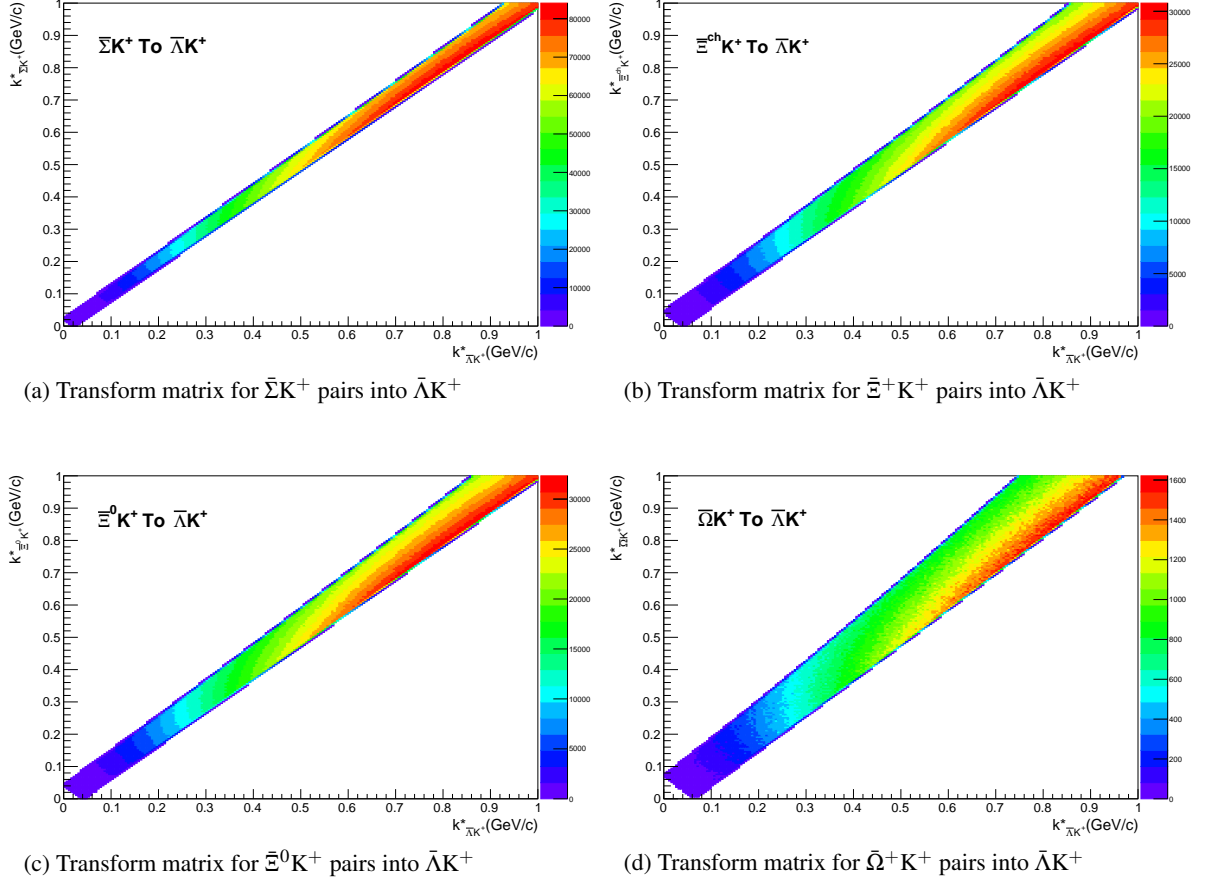


Fig. 3: Sample Transform Matrices generated with THERMINATOR for $\bar{\Lambda} K^+$ Analysis

parent system AB can be estimated using THERMINATOR as the total number of ΛK pairs originating from AB (N_{AB}) divided by the total number of ΛK pairs (N_{Total}):

$$\lambda_{AB} = \frac{N_{AB}}{N_{Total}} \quad (4)$$

Note, for our study, we consider a particle to be primary if its parent has a proper decay length of < 4 fm. The λ values used can be found in Table 1, for the case of both three and ten residual contributors. In the table, we also list the λ values used for “Other” and “Fakes”. The “Other” category contains pairs which are not primary, and which do not originate from the (3 or 10) residual pairs included in the fit. The “Fakes” category represents pairs that are mistakenly identified as ΛK . To estimate this λ_{Fakes} value, we assumed that the number of fake pairs was equal to the total number of pairs multiplied by the Λ purity (i.e. assuming perfect purity for the kaons); or, more simply, $\lambda_{Fakes} = 1.0 - \text{Purity}(\Lambda)$. For both of these contributors (“Other” and “Fakes”), we assume that these correlations average to unity, and therefore do not contribute to the final correlation function.

ΛK^+ residuals		$\bar{\Lambda} K^-$ residuals		ΛK^- residuals		$\bar{\Lambda} K^+$ residuals		ΛK_S^0 residuals		$\bar{\Lambda} K_S^0$ residuals	
Pair System	λ value	Pair System	λ value	Pair System	λ value	Pair System	λ value	Pair System	λ value	Pair System	λ value
3 Residuals											
ΛK^+	0.488	$\bar{\Lambda} K^-$	0.488	ΛK^-	0.487	$\bar{\Lambda} K^+$	0.489	ΛK_S^0	0.505	$\bar{\Lambda} K_S^0$	0.507
$\Sigma^0 K^+$	0.103	$\bar{\Sigma}^0 K^-$	0.102	$\Sigma^0 K^-$	0.102	$\bar{\Sigma}^0 K^+$	0.102	$\Sigma^0 K_S^0$	0.112	$\bar{\Sigma}^0 K_S^0$	0.111
$\Xi^0 K^+$	0.046	$\bar{\Xi}^0 K^-$	0.040	$\Xi^0 K^-$	0.046	$\bar{\Xi}^0 K^+$	0.041	$\Xi^0 K_S^0$	0.050	$\bar{\Xi}^0 K_S^0$	0.044
$\Xi^- K^+$	0.063	$\bar{\Xi}^+ K^-$	0.056	$\Xi^- K^-$	0.062	$\bar{\Xi}^+ K^+$	0.057	$\Xi^- K_S^0$	0.068	$\bar{\Xi}^+ K_S^0$	0.062
Other	0.252	Other	0.261	Other	0.255	Other	0.259	Other	0.217	Other	0.222
Fakes	0.048	Fakes	0.048	Fakes	0.048	Fakes	0.048	Fakes	0.048	Fakes	0.048
10 Residuals											
ΛK^+	0.317	$\bar{\Lambda} K^-$	0.319	ΛK^-	0.317	$\bar{\Lambda} K^+$	0.318	ΛK_S^0	0.342	$\bar{\Lambda} K_S^0$	0.344
$\Sigma^0 K^+$	0.105	$\bar{\Sigma}^0 K^-$	0.105	$\Sigma^0 K^-$	0.104	$\bar{\Sigma}^0 K^+$	0.106	$\Sigma^0 K_S^0$	0.113	$\bar{\Sigma}^0 K_S^0$	0.114
$\Xi^0 K^+$	0.047	$\bar{\Xi}^0 K^-$	0.042	$\Xi^0 K^-$	0.047	$\bar{\Xi}^0 K^+$	0.042	$\Xi^0 K_S^0$	0.051	$\bar{\Xi}^0 K_S^0$	0.045
$\Xi^- K^+$	0.064	$\bar{\Xi}^+ K^-$	0.058	$\Xi^- K^-$	0.063	$\bar{\Xi}^+ K^+$	0.059	$\Xi^- K_S^0$	0.069	$\bar{\Xi}^+ K_S^0$	0.063
$\Sigma^{*+} K^+$	0.049	$\bar{\Sigma}^{*-} K^-$	0.047	$\Sigma^{*+} K^-$	0.048	$\bar{\Sigma}^{*-} K^+$	0.048	$\Sigma^{*+} K_S^0$	0.052	$\bar{\Sigma}^{*-} K_S^0$	0.051
$\Sigma^{*-} K^+$	0.044	$\bar{\Sigma}^{*+} K^-$	0.046	$\Sigma^{*-} K^-$	0.044	$\bar{\Sigma}^{*+} K^+$	0.047	$\Sigma^{*-} K_S^0$	0.047	$\bar{\Sigma}^{*+} K_S^0$	0.050
$\Sigma^{*0} K^+$	0.044	$\bar{\Sigma}^{*0} K^-$	0.041	$\Sigma^{*0} K^-$	0.044	$\bar{\Sigma}^{*0} K^+$	0.042	$\Sigma^{*0} K_S^0$	0.047	$\bar{\Sigma}^{*0} K_S^0$	0.045
ΛK^{*0}	0.041	$\bar{\Lambda} \bar{K}^{*0}$	0.042	$\Lambda \bar{K}^{*0}$	0.041	$\bar{\Lambda} K^{*0}$	0.042	ΛK^{*0}	0.020	$\bar{\Lambda} \bar{K}^{*0}$	0.020
$\Sigma^0 K^{*0}$	0.037	$\bar{\Sigma}^0 \bar{K}^{*0}$	0.037	$\Sigma^0 \bar{K}^{*0}$	0.037	$\bar{\Sigma}^0 K^{*0}$	0.037	$\Sigma^0 K^{*0}$	0.017	$\bar{\Sigma}^0 \bar{K}^{*0}$	0.018
$\Xi^0 K^{*0}$	0.017	$\bar{\Xi}^0 \bar{K}^{*0}$	0.015	$\Xi^0 \bar{K}^{*0}$	0.017	$\bar{\Xi}^0 K^{*0}$	0.015	$\Xi^0 K^{*0}$	0.008	$\bar{\Xi}^0 \bar{K}^{*0}$	0.007
$\Xi^- K^{*0}$	0.022	$\bar{\Xi}^+ \bar{K}^{*0}$	0.021	$\Xi^- \bar{K}^{*0}$	0.022	$\bar{\Xi}^+ K^{*0}$	0.021	$\Xi^- K^{*0}$	0.011	$\bar{\Xi}^+ \bar{K}^{*0}$	0.010
Other	0.166	Other	0.174	Other	0.169	Other	0.171	Other	0.176	Other	0.181
Fakes	0.048	Fakes	0.048	Fakes	0.048	Fakes	0.048	Fakes	0.048	Fakes	0.048

Table 1: λ values for the individual components of the ΛK correlation functions for the case of 3 and 10 residual contributions.

Now, the remaining question is how do we model the parent correlation functions? In an ideal world, we would simply look up the parent interaction in some table, and input this into our Lednicky equation (for the case of one or more charge neutral particle in the pair), or run it through the CoulombFitter machinery described in Sec.???. Unfortunately, the world in which we live is not perfect, such a table does not exist, and little is known about the interaction between the residual pairs in this study. One solution would be to introduce a set of scattering parameters and radii for each residual system. However, as was the case of the λ -parameters above, this would introduce a large number of additional fit parameters, and would make our fitter too unconstrained and would yield untrustworthy results. The second option, which is adopted in this analysis, is to assume all residual pairs have the same source size as the daughter pair, and all Coulomb-neutral residual pairs also share the same scattering parameters as the daughter pair (the case of charged pairs, such as $\Xi^- K^\pm$ or $\Sigma^{*\pm} K^\pm$, will be described below).

Concerning the radii of the residual parent pairs, it was suggested that these should be set to smaller values than those of the daughter pair. In the interest of minimizing the number of parameters in the fitter, we tested this by introducing an m_T -scaling of the parents' radii. The motivation for this scaling comes from the approximate m_T -scaling of the radii observed in ???. To achieve this scaling, we assume the radii follow an inverse-square-root distribution: $R_{AB} = \alpha m_T^{-1/2}$. Then, it follows that we should scale the parent radii as:

$$R_{AB} = R_{\Lambda K} \left(\frac{m_{T,AB}}{m_{T,\Lambda K}} \right)^{-1/2} \quad (5)$$

The values of m_T for each pair system were taken from THERMINATOR. As the fitter dances around parameter space and selects a new radius for the ΛK system, the radii of the residuals is simply the ΛK radius scaled by the appropriate factor, given above (Eq.5). In the end, this scaling factor made no significant difference in our fit results, so this complication is excluded from our final results. Note that this is not surprising, as the most extreme scaling factor was, in the case of using 10 residual systems, between ΛK^+ with $m_{T,\Lambda K^+} \approx 1.4 \text{ GeV}/c^2$ and $\Xi^- K^{*0}$ with $m_{T,\Xi^- K^{*0}} \approx 1.8 \text{ GeV}/c^2$, resulting in a scale factor of ≈ 0.9 .

Now, as hinted above, accounting for charged residuals adds a complication in that they necessitate the inclusion of the CoulombFitter (described in Sec. ??) into the process. The complication of combining the two fitters is not troubling; however, the substantial increase in the fitting time is (the parallelization of the CoulombFitter across a large number of GPU cores, to drastically decrease run-time, is currently underway). We have two solutions to bypass such a large increase in run time. First, we can use our experimental $\Xi^{\text{ch}} K^{\text{ch}}$ data to represent all charged parent pair system. In this case, there is no need to make any assumption about scattering parameters or source sizes, as we already have the experimental data. The downside is that, especially in the 30-50% centrality bin, the statistics are low and error bars large. Alternatively, we can assume the strong interaction is negligible in the charged residual, and generate the parent correlation function given radius and λ parameters. We find in our $\Xi^{\text{ch}} K^{\text{ch}}$ study that a Coulomb-only description of the system describes, reasonably well, the broad features of the correlation. The strong interaction is necessary for the fine details. However, as these correlations are run through a transform matrix, which largely flattens out the fine details, a Coulomb-only description should be sufficient. In practice, this Coulomb-only scenario is achieved by first building a large number of Coulomb-only correlations for various radii and λ parameter values, and interpolating from this grid during the fitting process. We find consistent results between using the ΞK data and the Coulomb-only interpolation method. When quantifying the $\Xi^- K^\pm$ residual contribution, the experimental $\Xi^- K^\pm$ data is always used. When the number of residual pairs used is increased to 10, so that contributors such as $\Sigma^{*+} K^-$ enter the picture, the Coulomb-only interpolation method is used. In other words, the ΞK experimental data is only used to model the ΞK residual contribution, all other charged pairs are treated with the Coulomb-only interpolation method.

Two examples of how very different transform matrices can alter a correlation function are shown in Figures 4 and 5 below. These figures were taken using parameter values obtained from fits to the data. In the top left corner of the figures, the input correlation function (closed symbols) is shown together with the output, transformed, correlation function (open symbols). In the bottom left, the transformed correlation is shown by itself (with zoomed y-axis). This is especially helpful when the λ parameter is very small, in which case the contribution in the top left can look flat, but the zoomed in view in the bottom left shows the structure. The right two plots in each figure show the transform matrix without (top right) and with (bottom right) a log-scale on the z-axis. Note, more examples of these transforms can be found in Sec. ??.

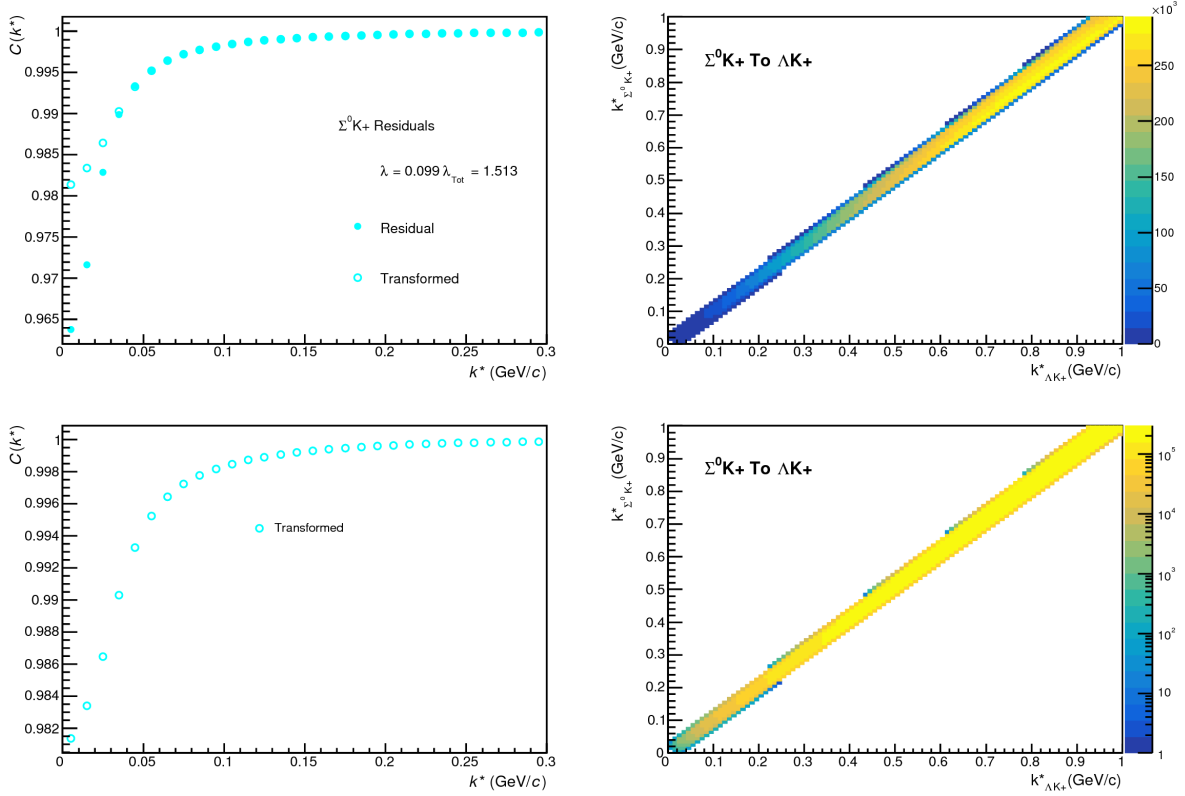


Fig. 4: $\Sigma^0 K^+$ Transform. These figures were taken using parameter values obtained from fits to the data. In the top left corner of the figures, the input correlation function (closed symbols) is shown together with the output, transformed, correlation function (open symbols). In the bottom left, the transformed correlation is shown by itself. The right two plots in each figure show the transform matrix without (top right) and with (bottom right) a log-scale on the z-axis.

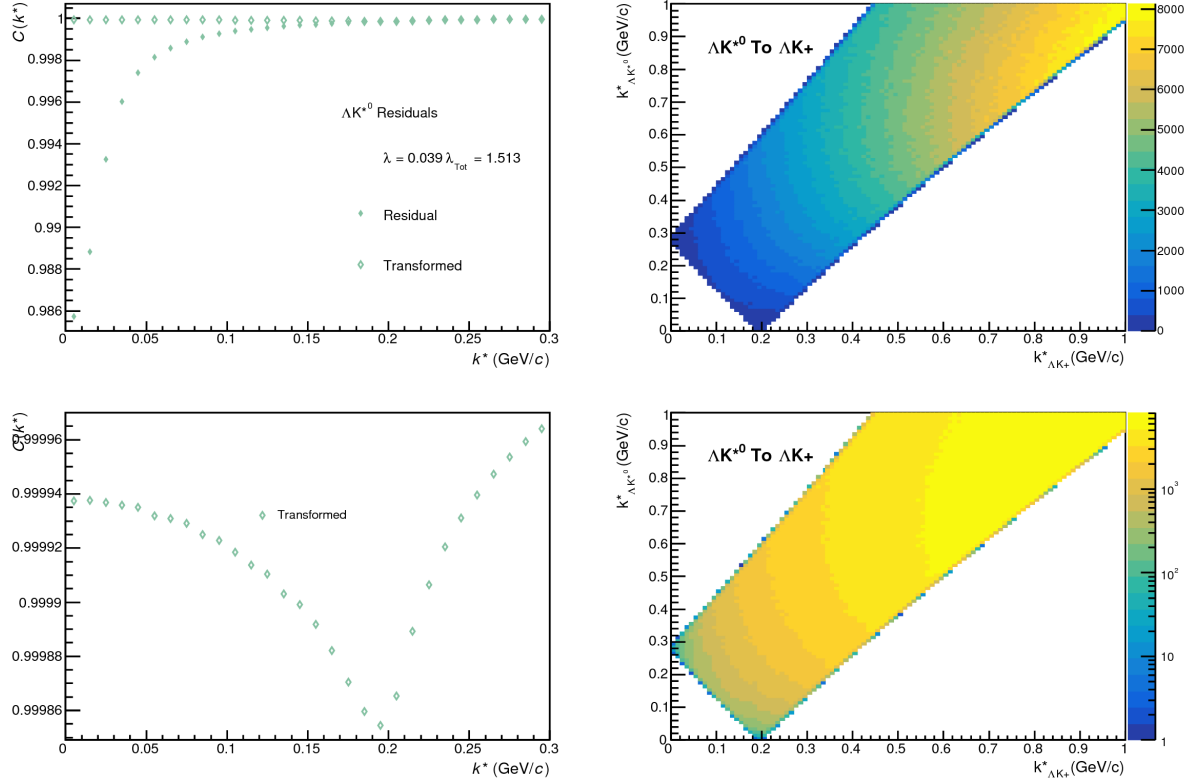


Fig. 5: ΛK^{*0} Transform. These figures were taken using parameter values obtained from fits to the data. In the top left corner of the figures, the input correlation function (closed symbols) is shown together with the output, transformed, correlation function (open symbols). In the bottom left, the transformed correlation is shown by itself. The right two plots in each figure show the transform matrix without (top right) and with (bottom right) a log-scale on the z-axis.